LA-UR-16-27553
Approved for public release; distribution is unlimited.

Title: Constituent Redistribution in U-Zr Metallic Fuel Using the Advanced Fuel Performance Code BISON

Author(s): Galloway, Jack D.
Unal, Cetin
Matthews, Christopher

Intended for: Report

Issued: 2016-09-30

LA-UR-16-XXXXXX

Constituent Redistribution in U-Zr Metallic Fuel Using the Advanced Fuel Performance Code BISON

Jack Galloway
Cetin Unal
Christopher Matthews

September 2016

Introduction

Previous work done by Galloway, et. al. [1] on EBR-II ternary (U-Pu-Zr) fuel constituent redistribution yielded accurate simulation data for the limited data sets of Zr redistribution. The data sets included EPMA scans of two different irradiated rods. First, T179 which was irradiated to 1.9 at% burnup was analyzed. Second, DP16 which was irradiated to 11 at% burnup was analyzed. One set of parameters that most accurately represented the zirconium profiles for both experiments was determined. Since the binary fuel (U-Zr) has previously been used as the driver fuel for sodium fast reactors (SFR) as well as being the likely driver fuel if a new SFR is constructed, this same process has been initiated on the binary fuel form. From limited binary EPMA scans as well as other fuel characterization techniques, it has been observed that zirconium redistribution also occurs in the binary fuel, albeit at a reduced rate compared to observation in the ternary fuel, as noted by Kim et. al. in [2]. While the rate of redistribution has been observed to be slower, numerous metallographs of U-Zr fuel, such as the one shown in Figure 1, show distinct zone formations.

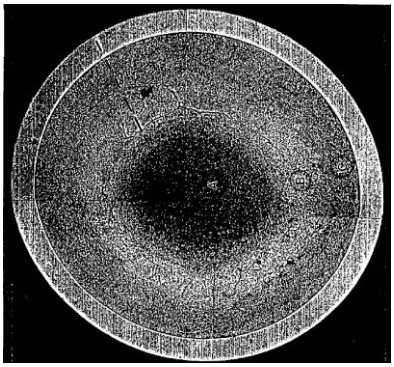

Figure 1 - Fuel rod DP81 metallograph showing distinct phase separation

Additionally limited EPMA scans confirm these visual inspections, showing a zirconium rich rod center, zirconium depleted mid-radius and a nearly unchanged outer radius. Figure 2 shows one such scan corresponding to rod DP81 seen in Figure 1.

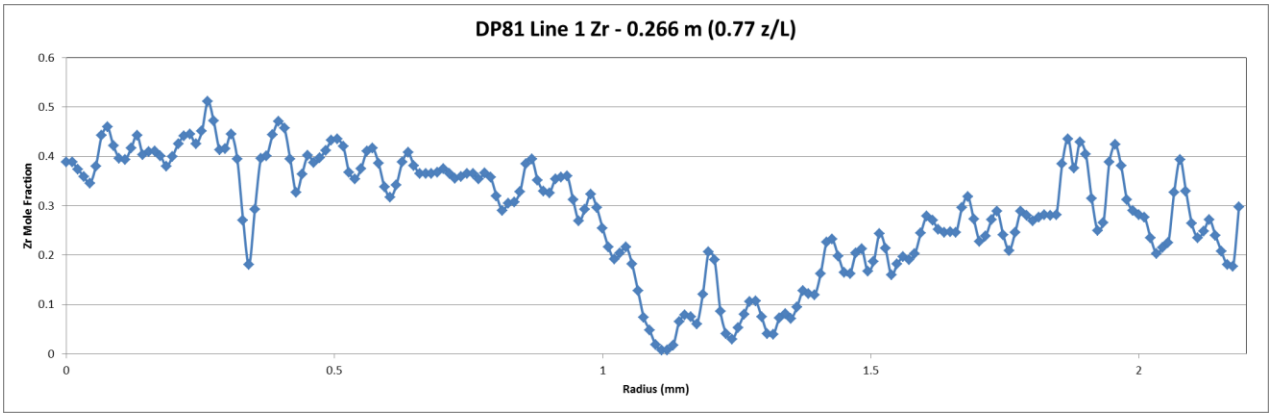

Figure 2 - EPMA scan of Zr redistribution for rod DP81

Available Data (DP11 and DP81)

Few EPMA scans such as the one shown in Figure 2 exist. The two datasets for U-Zr currently available come from rods DP11 and DP81, both irradiated in subassembly X447A in EBR-II with an HT-9 cladding. DP11 was irradiated to 10 at% burnup at high cladding temperatures [3]. One EPMA scan was obtained very near the top of the rod (0.95 z/L). DP81 was irradiated in the same EBR-II subassembly to 5 at %. Three EPMA scans were obtained, two at the same axial level very near the top of the rod (0.94 z/L) and one scan near three quarters length of the rod axially (0.77 z/L) [4]. These scans, with one example of the obtained dataset shown here in Figure 3, were analyzed using a utility for converting scanned data to numerical form, with the corresponding data from the plot being the data plot in Figure 2.

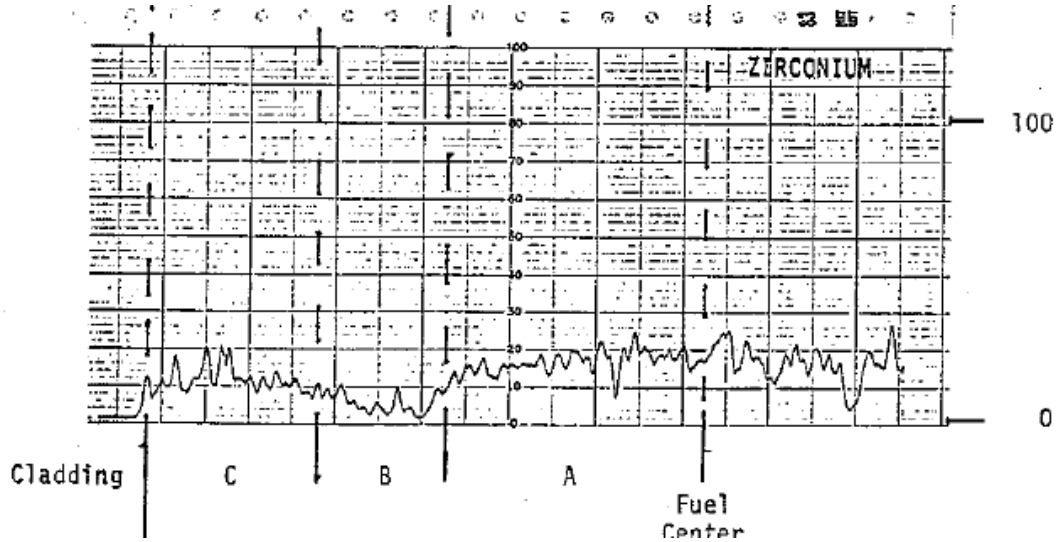

Figure 3 - DP81 EPMA scan as reported in [4]

Zirconium redistribution input decks were created that followed the EBR-II declared operating data. Table 1 shows important input parameters used for the DP81 and DP11 simulations. The axial power profile used to scale the overall rod average power is shown in Figure 4 and the time dependent power profile is shown in Figure 5. Note that the irradiation times for DP11 also included those for DP81.

Table 1 - DP11 & DP81 input parameters

Fuel slug radius (cm)	0.216
Fuel slug density (g/cm3)	15.8
Fuel smeared density (%)	72.3
Fuel-cladding gap material	Liquid Na
Cladding thickness (cm)	0.0381
Fuel-cladding gap width (cm)	0.0762
Fuel length (cm)	34.29
Coolant temp (inlet - C)	380
Mass flux (kg/m^2-sec)	2437.77

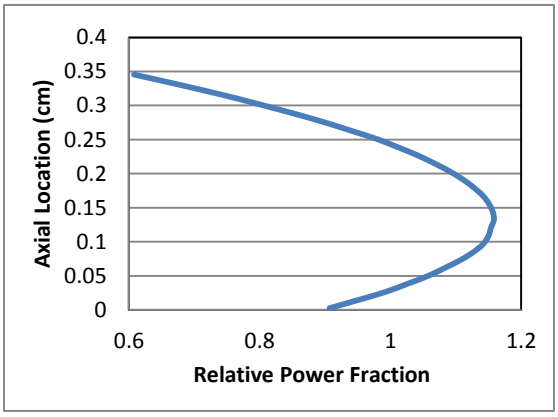

Figure 4 - DP11 & DP81 Axial Power Profile

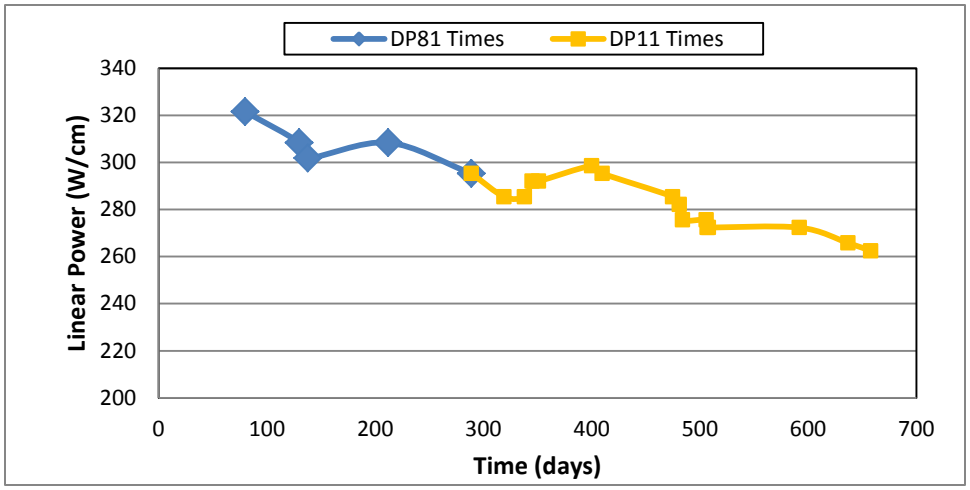

Figure 5 - DP11 & DP81 Linear Power History

U-Zr Phase Diagram

The most important aspect of modeling constituent redistribution is the phase diagram. Whereas the ternary system had a complex phase diagram, simplified to a pseudo-binary phase diagram using the assumption of sessile Plutonium [1], the U-Zr system has a less complex phase diagram. Figure 6 shows a phase diagram for U-Zr fuel.

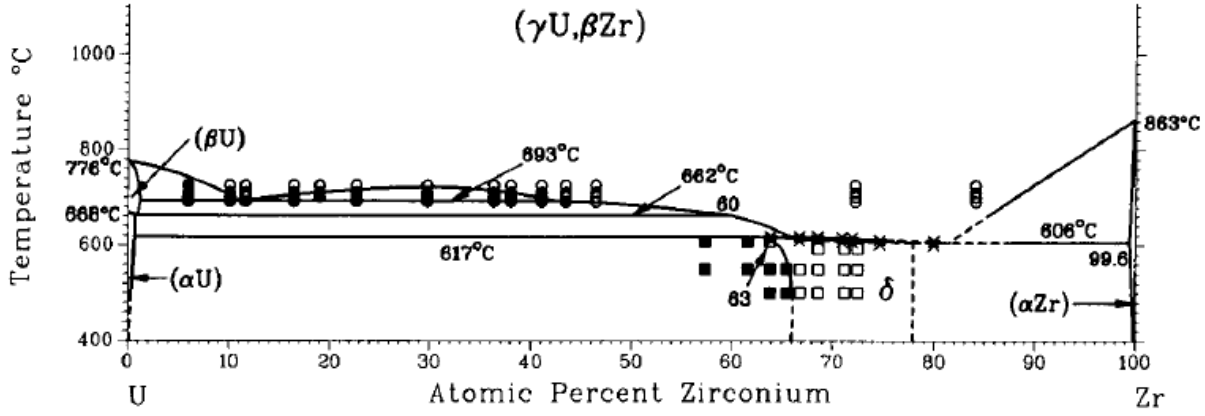

Figure 6 - U-Zr Experimental Phase Diagram [5]

However, as was the case with the previously conducted ternary analysis, the locations of the phase transitions observed in the EPMA scans do not come close to expected locations from the equilibrium phase diagram shown here when a thermal solution is performed using operating conditions. Thus the phase diagram temperature transitions are used as an input parameter to adjust. Figure 7 shows an example of an amended phase diagram, highlighting some of the simplifications, as well as the shift required in the temperature transitions to obtain observed zirconium redistribution behavior.

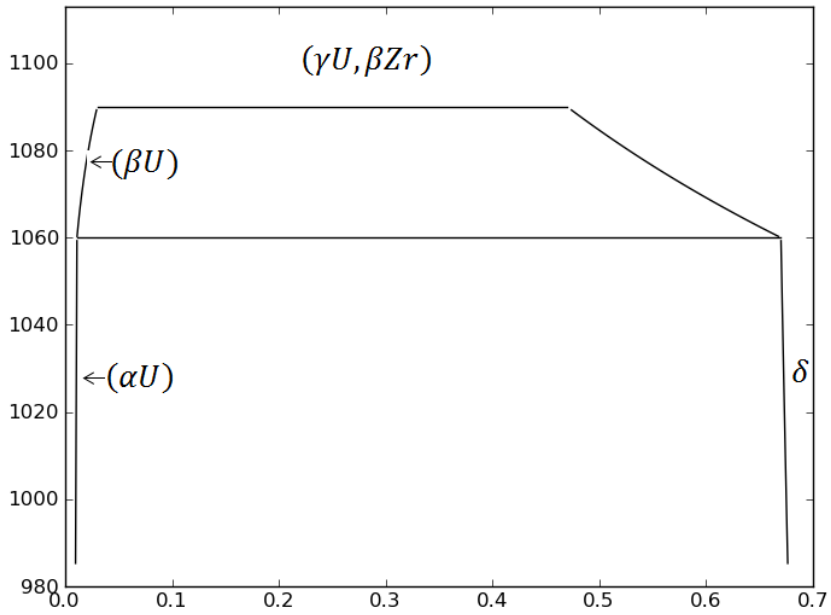

Figure 7 - U-Zr Simulation Phase Diagram Example

The first simplification to note is the collapsing of the αU and βU phases into a single βU phase above the first transition temperature (617 °C according to Figure 6). Where there used to be two delineating regions of αU at 617 and 662 °C as a result of changing Zr phases at these temperatures, then to βU above 662 °C up to the γ transition temperature of 693 °C. In place of the more complicated phase diagram, a single phase that is treated as βU is accounted used for both the αU and βU above the 617 °C phase transition. This simplification is made due to the currently available phase diagram evaluation kernels as well as the observation that both αU and βU behave in a similar fashion, having the same positive sign on the heat of transport. Should the differences between these two phases be found extremely important, additional complexity to the diffusion kernel may be included. The second item of note is that the transition temperatures moved up significantly. The original temperature transitions captured occurred at 890 K (617 °C) and 966K (693°C). They have now been adjusted to 1060 K and 1090 K for this representative diagram. Thus increases by more than 100 K were required to obtain zirconium distributions that were at least starting to represent the EPMA data; a similar result to the initial U-Pu-Zr work. It should be noted that while this phase diagram is used as a representative example, this phase diagram is not being claimed as the recommended phase diagram for irradiated U-Zr simulations but as a representative plot highlighting the large adjustments necessary.

U-Zr Constituent Redistribution Results

A determination of recommended parameters for phase dependent (α, δ, β, γ) diffusion coefficients and phase diagram parameters (transition temperatures) is currently underway. Emulating the process from previous work in determining these parameters for U-Pu-Zr fuel, an analogous iterative process has been undertaken. This process involves first determining parameters that match the shorter irradiated DP81 experiment, applying them to the longer irradiated DP11 experiment, then iterating back and forth

until one set of parameters best estimates both experiments. Once this is completed, the parameters will then be applied to a third case not used in the optimization scheme which serves as an independent assessment of the accuracy of the optimized parameters. Initial simulations are performed on a single level (1D) simulation to assess optimum parameters. Subsequently the parameters are then applied to a full length 2D-RZ simulation that captures axial effects as well. This process is still underway and the current results represent a reporting of the current status and detailing what remains to be done.

1D Simulation

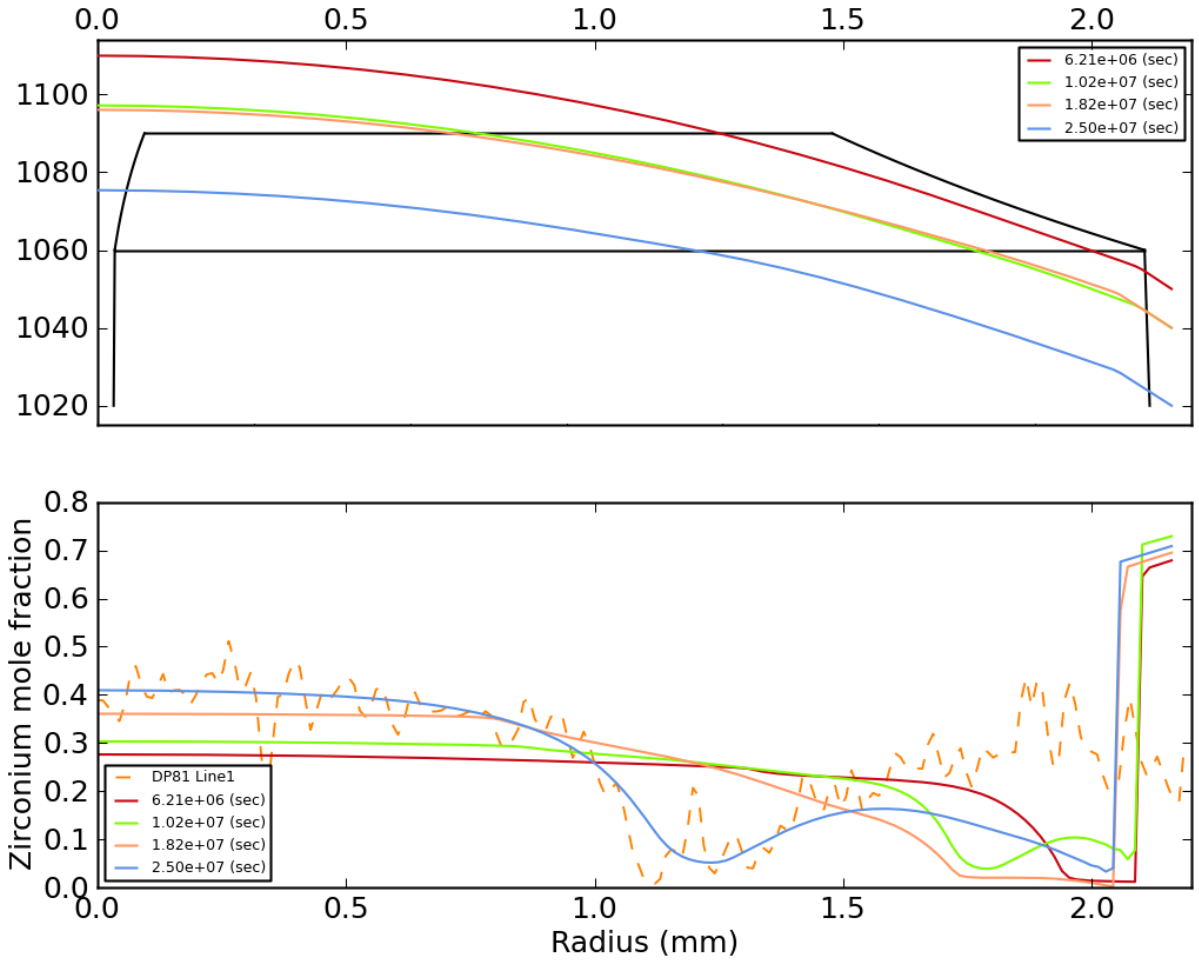

Figure 8 - DP81 Simulation at 0.77 z/L. phase diagram and zirconium redistribution

Figure 8 shows the culmination of several thousand 1D simulations which enveloped a large number of combinations of temperature transitions and phase dependent diffusion coefficient combinations. The top graph overlays temperatures at various points in time, which correspond to power changes, on top of the prescribed phase diagram. The axis on top and bottom correspond to the radial distance. The temperature overlays highlight the necessity of temperature transitions corresponding to abrupt changes in the zirconium redistribution profile. Thus the abrupt change in zirconium concentration near 1.0 mm and 1.4 mm are a result of temperature changes at these locations. Observing the calculated

temperature distribution helps gauge the magnitude of the temperature transition. However, one cannot simply simulate the thermal solution apart from zirconium redistribution and take that as the de facto temperature transition. As the zirconium redistributes, the uranium profile follows as the inverse of the zirconium, which then redistributes the power profile according to the local uranium concentration. Thus as the zirconium redistributes so does the power profile which will cause shifts in the overall temperature solution. Since this is a secondary effect, a representative thermal solution can help inform the starting point from which to vary temperature transitions. Additionally, the temperature and phase diagram co-plot should be used only to estimate expected transition temperatures, since the actual zirconium concentration is not also considered in the plot.

Observed in Figure 8 is that at end-of-life (EOL) for rod DP81, the zirconium distribution matches the data well at rod center and mid-radius, including capturing the correct transition locations. However still under investigation is the zirconium behavior at rod edge. Since the rod experiences higher power early in life, hotter conditions exist which result in material phases that are nearly exclusively single phase γ or two-phase β-γ with a very small fraction of two-phase α-δ near the rod edge. This results in sweeping the zirconium out of the two-phase β-γ phase since the γ contribution drives the zirconium up the temperature gradient and the β contribution sweeps down the temperature gradient. As the power decreases over the life of the DP81 fuel pin, the temperature distribution also decreases. Observed in both the green and orange data lines, which represent very slight power changes, is still a phase dominance of single phase γ or two-phase β-γ and a larger, yet still minority contribution of two-phase α-δ. Thus again the two-phase β-γ sweeps the zirconium out towards rod center or rod edge, creating the local minimum concentration of 0.02 zirconium mole fraction. Furthermore the significant spike in zirconium concentration at rod edge does not appear to be physically representative. The occurs because of the boundary condition imposed at the rod edge, along with the tendency for the α-δ phases to both preferentially drive zirconium down the temperature gradient. While the zirconium gradient is set to zero at this boundary, there is still a Soret term which imposes a flux term at the edge. This is clearly seen in equation 1.15 from [1].

$$\frac{\partial x}{\partial t} = \nabla \cdot D(x,T)\nabla x + \nabla \cdot S(x,T)\nabla T \qquad (1.15)$$

While the ∇x term is set to zero, the overall $\frac{\partial x}{\partial t}$ term still has a meaningful value at the outer boundary since ∇T is non-zero at rod edge. Obviously the $\frac{\partial x}{\partial t}$ term is zero at rod center since both ∇T and ∇x are zero. Further investigation into a more physically representative boundary condition is needed. Interestingly, in the work for the U-Pu-Zr fuel this rod edge effect was observed, albeit it a smaller magnitude. This is believed to be due, in part, to a limiting coefficient on the Soret term, dependent on the plutonium concentration. See equation 1.17 from [1] below.

$$S(x,T) = D_\pi(x,T)\left(\frac{x(1-x_{\mathrm{Pu}}-x)}{1-x_{\mathrm{Pu}}}\right)\frac{Q_\pi^\star}{RT^2}, \qquad (1.17)$$

The $\frac{x(1-x_{Pu}-x)}{(1-x_{Pu})}$ term serves to slow the Soret driven effect at rod edge according to the amount of Pu in the problem. In the case of U-Zr fuel, where there is no Pu the Soret term at rod edge will tend to be faster. The development and implementation of a boundary condition which limits $\frac{\partial x}{\partial t}$ to zero at the specified boundary would perhaps ameliorate this problem.

2D-RZ Simulation

Full length, 2D-RZ simulations of DP81 were also performed. In place of a fixed temperature boundary condition on the outside of the fuel, as was utilized in the 1D simulations, a convective heat transfer solution dependent on the coolant inlet temperature, mass flux and other required geometric parameters was performed. One difficulty encountered when simulating the full length surrounds the parameters controlling artificial diffusion in the two-phase regimes. Recalling the necessity of artificial diffusion in the two-phase region is first required [1]:

> "In a 2-phase region one ought to take D = 0, however this would result in Eq. (1.15) being purely advective with a transport velocity proportional to the temperature gradient. Mathematically this leads to jump discontinuities in the Zr atom fraction profile at domain boundaries and boundaries between single and 2-phase regions. Moreover, it is well-known that standard centered finite difference or Galerkin finite element schemes are unstable for pure advection, leading to spurious oscillations. Thus to stabilize our Galerkin finite element implementation we add some artificial diffusion and take:
>
> $$D(x,T) = f_\beta D_\beta(X_\beta(T),T)p_\beta + (1-f_\beta)D_\gamma(X_\gamma(T),T)p_\gamma, \qquad (1.19)$$
>
> where p_β and p_γ are dimensionless numerical parameters takenas small as possible while maintaining stability."

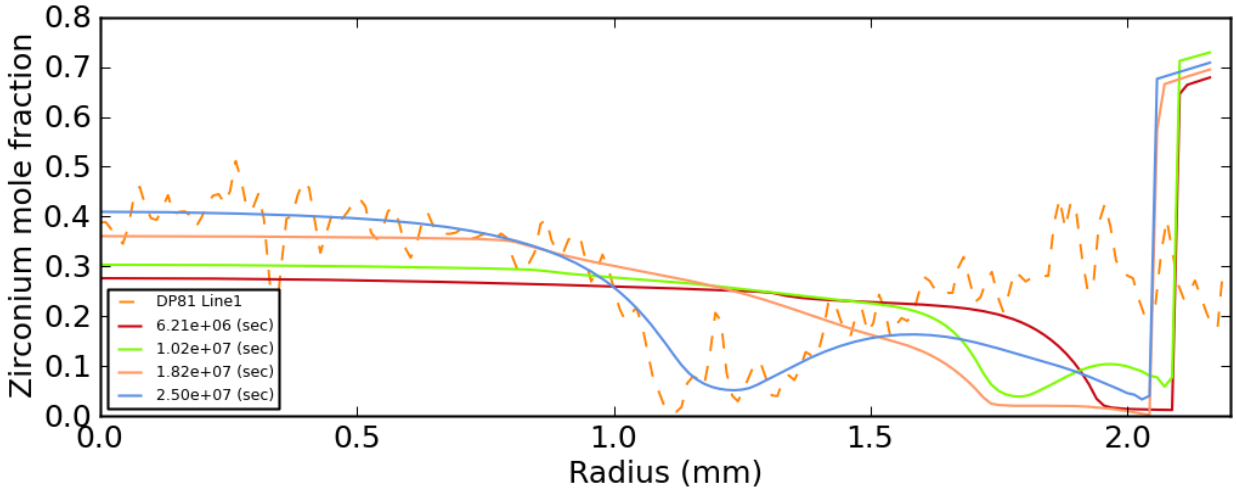

Figure 9 - 1D simulation, p-values of 0.01

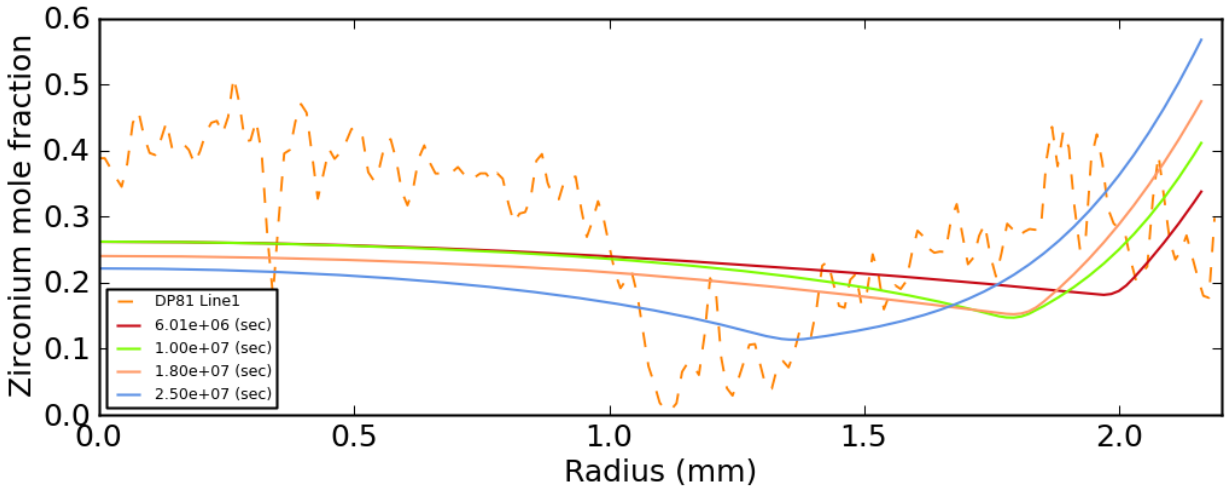

Figure 10 - 1D simulation, p-values of 0.4

Thus, while not desired from a phenomenological standpoint the p-values are necessary for numerical stability. When desiring to take these values as small as possible there is no appreciable computational penalty when performing 1D simulations due to the small mesh and relatively simpler model for boundary conditions and convergence. However, using too small of values in the 2D-RZ simulations causes long run times due to very small time step sizes. Yet, when using larger p-values the results can have significant changes. Take for instance the following two 1D simulations using p-values of 0.01 and 0.4, seen in Figure 9 and Figure 10 respectively. At two different p-values the results are drastically different. One set of diffusion coefficients that match the data well with p-values of 0.01 do not match well with p-values of 0.4. An easy conclusion is to use p-values of 0.01 or smaller, since we believe the smaller the p-value the more representative of reality the solution is. This is problematic since using p-values of 0.01 in a full length 2D-RZ simulation results in time steps of ~250 seconds, which can be extraordinarily penalizing when simulations consist of large meshes and simulations out to 2.5E7 seconds requiring nearly 100,000 time steps. While a confirmatory analysis is underway for p-values of 0.01, a full length 2D-RZ simulation was run using the convective heat transfer boundary condition and p-values of 0.4 to compare simulation results. Figure 11 shows the 2D-RZ results. The results look nearly identical to the 1D result. While awaiting the confirmatory analysis for the case of p-values being 0.01, this is an advantageous finding. Assuming the simulation at 0.01 shows the same result, with 2D-RZ results and 1D results being nearly identical for the same p-values, it means the iterative process can be performed on small, fast running simulations. Of course down the road when applying the optimized parameters to problems, accommodations for run time will have to be made either through clever application of the kernel in the 2D problem, or by leveraging advanced numerical techniques to move beyond the p-value approximation. In assessing the impact of the p-values on simulation results, an analysis of equation 1.15 from [1], shown above, when considering single phase versus two-phase regimes is helpful. In single phase regimes equation 1.15 shows both the diffusive, concentration gradient driven term and the Soret, temperature driven term. Given that both concentration and temperature gradients exist in the single phase regime, there is no need for artificial diffusion, thus p-values. Conversely in the two-phase regime, where it should be driven purely by the temperature

gradient, and the concentration driven term should be set to zero, yet a concentration driven diffusion term is needed for stability. Thus problems that consist mainly in single phase regions, or that quickly evolve into single phase regions, will be less sensitive to the p-values. In contrast, for problems that exist primarily in the two-phase domain the sensitivity to the p-values will be much higher.

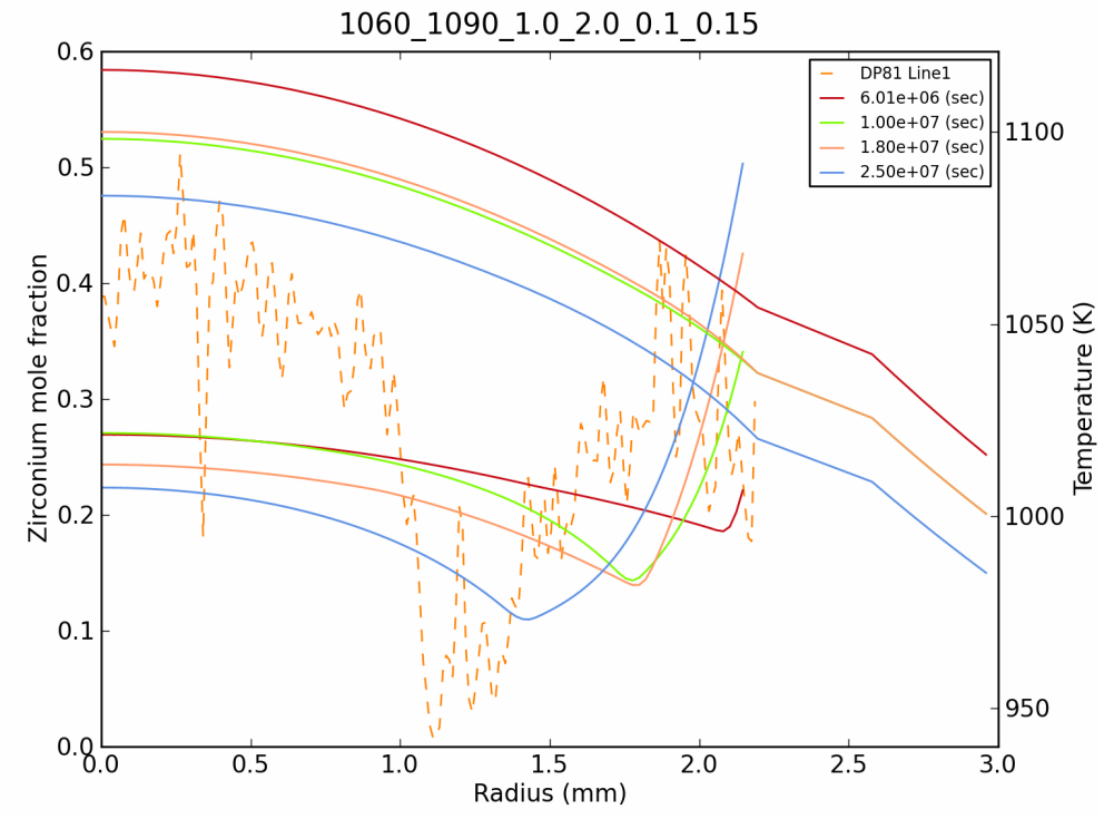

Figure 11 - 2D-RZ simulation, p-values of 0.4

Conclusions & Future Work

An evaluation of U-Zr metallic fuel constituent redistribution is progressing. Three experimental data sets from two different EBR-II rods are being utilized in the iterative scheme. Values for the phase diagram, diffusion coefficients and p-values have been obtained that match the data for the first experiment, DP81, reasonably well using 1D simulations. Additionally the 1D simulation approach has been partially validated in a 2D-RZ calculation using higher p-values, thus higher artificial diffusion in the two-phase regions. This confirmatory study between 1D and 2D-RZ simulations is being re-examined using the optimized diffusion coefficients, phase diagram and lower p-values. Once this confirmation is completed, assuming the 1D and 2D-RZ results agree at low p-values, work on evaluating one set of parameters that predicts both DP81 and DP11 as accurately as possible will continue. When this is completed a third application, preferably to another EBR-II rod where a clear delineation of phase transition locations is observable to assess phase transition behavior is needed. Additional work in implementing advanced numerical schemes for advective solutions, or implementation of advanced predictive models for axially and radially varying p-values which preserve simulation accuracy would be valuable for both accuracy and expediency in the simulation of larger problems. Additional useful experimental work to aid the development of computational models would be continued destructive analysis of historical SFR metallic rods, both U-Zr and U-Pu-Zr, to provide more quantitative datasets to include in assessing and refining the model. Experimental efforts leveraged toward quantifying phase specific properties, such as diffusion coefficients would be useful in reducing the number of unknown, and thus variable, parameters in the constituent redistribution solution.

References

[1] J. Galloway, C. Unal, N. Carlson, D. Porter and S. Hayes, "Modeling constituent redistribution in U-Pu-Zr metallic fuel using the advanced fuel performance code BISON," *Nuclear Engineering and Design,* vol. 286, pp. 1-17, 2015.

[2] Y. S. Kim, G. L. Hofman, S. L. Hayes and Y. H. Sohn, "Constituent redistribution in U-Pu-Zr fuel during irradiation," *Journal of Nuclear Materials,* vol. 327, no. 1, pp. 27-36, 1 April 2004.

[3] R. V. Strain, "Destructive examinatino of fuel pin DP11, X447A at the alpha gamma hot cell facility, ANL-E," Argonne National Laboratory, Argonne, IL, 1993.

[4] J. E. Sanecki, "Results of electron microprobe examination of two specimens taken from IFR fuel element DP-81," Argonne National Laboratory, Argonne, IL, 1991.

[5] R. I. Sheldon and D. E. Peterson, "The U-Zr (Uranium-Zirconium) System," *Bulletin of Alloy Phase Diagrams,* vol. 10, no. 2, 1989.